Large-Scale Cellular Coverage Analyses for UAV Data Relay via Channel Modeling

Yaguang Zhang, Tomohiro Arakawa, James V. Krogmeier,
Christopher R. Anderson, David J. Love, and Dennis R. Buckmaster

***Abstract*—With the rapid popularity of unmanned aerial vehicles (UAVs) such as drones, extending wireless communication coverage via UAV data relay, especially for rural areas, becomes cost-effective. Its flexibility attracts research attention from a variety of areas, including Internet of Things, intelligent transportation systems, and digital agriculture. However, most current research effort focuses on modeling small-scale data relay systems and theoretically optimizing the system performance via UAV trajectories, while the decision of taking advantage of UAVs for real-life wireless communication networks requires large-scale quantitative performance analysis results based on practical environment information. In this paper, we propose algorithms for generating large-scale blockage and path loss maps via terrain-based channel modeling for cellular communication systems with relay drones. Our analyses reveal the coverage ratios for Tippecanoe County, Indiana, with relay drones simulated at different heights. The area of interest is also extended to include all ten counties in the Wabash Heartland Innovation Network (WHIN). For both cases, a coverage ratio gain over 40% can be achieved at a drone height of 100 m, compared to a typical pedestrian height of 1.5 m. These site-specific analyses are important in locating poorly covered spots and quantifying the possible improvement from UAV data relay.**

***Index Terms*—Cellular coverage analysis, data relay, site-specific channel modeling, unmanned aerial vehicles.**

I. Introduction

The rapid development of unmanned aerial vehicle (UAV) technologies has provided a vast array of new possibilities for wireless communications [1]. In particular, consumer-grade drones debuted around a decade ago and have become increasingly sophisticated for a lower cost. These drones have demonstrated the ability to dramatically alter several industries [2]. Boosted by advanced technologies like energy-efficient autonomous target tracking [3], the popularity of drones is making it possible and cost-effective to extend wireless communication coverage via UAV data relay, especially for rural areas where network coverage is sparse or nonexistent [4]. The flexibility of UAV-aided wireless communication has attracted research attention from a variety of areas, including Internet of Things [5], intelligent transportation systems [6], and digital agriculture [7]. On-demand deployment of relay UAVs may play a key role in improving mobile service quality in many challenging scenarios faced by today's communication infrastructure. However, most current research efforts focus on modeling small-scale data relay systems and theoretically optimizing the system performance via UAV trajectories [8]–[10], while the decision of deploying UAVs in real-life wireless communication networks requires large-scale quantitative performance analysis results based on practical environment information.

To fill this research gap, we propose algorithms for generating large-scale blockage and path loss maps via terrain-based channel modeling for cellular communication systems with relay drones. Based on high-resolution LiDAR data, the blockage maps are used to locate regions with line-of-sight (LoS) obstruction and identify areas that may benefit from utilizing UAV data relay. Simultaneously, the path loss maps store path loss values calculated from terrain elevation data, enabling us to discover regions with satisfactory coverage conditions and quantify the system performance. These algorithms were applied to Tippecanoe County, Indiana, with relay drones simulated at different heights to obtain the overall coverage gains of implementing UAV-aided cellular communication systems. Furthermore, we were able to extend the area of interest to include ten counties [11] in the Wabash Heartland Innovation Network (WHIN), Indiana, for carrying out similar cellular coverage analyses. A significant coverage ratio gain of over 40% can be achieved for both cases at a drone height of 100 m. Regions which would benefit the most were also revealed by the resulting maps. These site-specific analyses are important for quantifying the possible improvement from UAV data relay and guiding the implementation of such systems.

Our work makes the following contributions: (i) it provides quantitative analyses for UAV data relay at system level over a large geographic area, (ii) blockage detection is computed using publicly available LiDAR data as an effective alternative to full propagation simulation, and (iii) the coverage ratio gain over different path loss values is introduced to link the benefit of UAV data relay systems to quality-of-service metrics. The paper is organized as follows. In Section II, we present our algorithms for generating blockage and path loss maps. Coverage analyses based on these maps are described in Section III. Finally, in Section IV, we conclude the paper.

II. Terrain-Based Channel Modeling

A. Scenario Model

Consider the scenario illustrated in Fig. 1. An agricultural end user is operating in a region with sparse coverage. A dedicated UAV follows the user at a constant height above ground h_D to act as a relay between the user and remote cell towers serving the area of interest. The communication between the

Y. Zhang, T. Arakawa, J. V. Krogmeier, and D. J. Love are with the School of Electrical and Computer Engineering, Purdue University, 465 Northwestern Avenue, West Lafayette, IN 47907, USA. (Email: {ygzhang, tarakawa, jvk, djlove}@purdue.edu)

C. R. Anderson is with the Department of Electrical and Computer Engineering, United States Naval Academy, 105 Maryland Ave, Annapolis, MD 21402, USA. (Email: canderso@usna.edu)

D. R. Buckmaster is with the College of Agriculture, Purdue University, 615 West State Street, West Lafayette, IN 47907, USA. (Email: dbuckmas@purdue.edu)

Sponsorship for this work was provided by the Foundation for Food and Agriculture Research (award 534662) and the NSF (grant CNS-1642982).

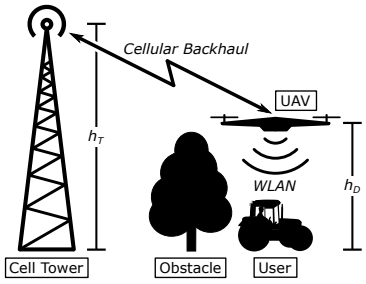

Fig. 1. Illustration of a typical UAV data relay scenario.

UAV and the user is assumed to be reliably taken care of by wireless local-area-network (WLAN) technology. This is a typical application in digital agriculture where the relay UAV provides extended communication links in rural areas for the user via a cellular backhaul. It can be easily observed that the relay UAV's presence allows the cell tower to reach some areas blocked at the user level. We are interested in modeling this improvement quantitatively at a large geographic scale for different values of h_D using freely-available geographic information such as LiDAR and terrain elevation data.

Such a data relay system can be conveniently implemented with very low cost by attaching a custom-configured cell phone to a modern photography drone with autonomous target tracking functionality. Compared to enhancing coverage via a vast amount of traditional repeaters or small cell systems, this approach provides the flexibility to enable inexpensive on-demand deployment of wireless communication infrastructure. The relay UAVs can be dispatched from the mobile service providers or set up privately on the user's side, and dismissed when they are no longer needed. This flexibility is the key to satisfy the intermittent connectivity requirement over a vast low-population area in many digital agriculture applications, including but not limited to scheduled sensor data collection and temporary data transmission during short-term activities such as planting and harvesting, without the high cost of building out traditional fixed infrastructure.

B. Simulation Scene Construction

The simulation was carried out primarily in the Universal Transverse Mercator (UTM) coordinate system. Conversions between UTM (x, y) and GPS $(latitude, longitude)$ were performed when necessary with a fixed UTM zone label *16T*. To incorporate the height dimension over a large geographic area, the UTM system is extended with $altitude$, the sum of the ground $elevation$ and the object height. The information needed for constructing the simulation scene includes the cell tower antenna locations and the drone locations to inspect. Our simulator, together with the coverage analysis algorithms, were implemented[1] using MATLAB R2019b.

1) Locating Effective Cell Towers: Cell tower GPS locations were obtained from a randomized U.S. cellular laydown used in a National Telecommunications and Information Administration (NTIA) analysis for Advanced Wireless Services (AWS)-3 spectrum sharing. This dataset contains real-life cell tower locations intentionally randomized with errors at a scale of a few kilometers for safety and privacy concerns. To reduce the number of cell towers considered in the simulation, we extended the area of interest by an estimated maximum cell tower coverage radius and only considered towers within that range, as illustrated in Fig. 2. Cell towers out of the extended area were considered ineffective and ignored in the corresponding simulation. For simplicity, the maximum coverage radius R_{Max} in kilometer was estimated as the longest optical horizon distance from the cell tower antenna:

$$R_{Max} \approx 3.57 \times \left(\sqrt{h_T} + \sqrt{h_D}\right), \tag{1}$$

where h_T and h_D are the heights in meter for the cell tower antenna and the drone, respectively. The antenna heights for all cell towers were set to be a typical value of 50 m in the simulation. For R_{Max}, we set $h_D = 1.5$ m, the lowest drone height inspected, which gave us $R_{Max} \approx 29.6$ km.

2) UAV Location Grid Construction: A grid for the UAV locations covering the area of interest was built for each simulation, as shown in Fig. 3. Its spatial resolution is determined by the number of grid points N_{Samp} for the longer side (width or height) of the area of interest. We had $N_{Samp} = 100$ (over 38.5 km) for Tippecanoe County and, to compensate the extra cell towers to consider, $N_{Samp} = 50$ (over 144.8 km) for the

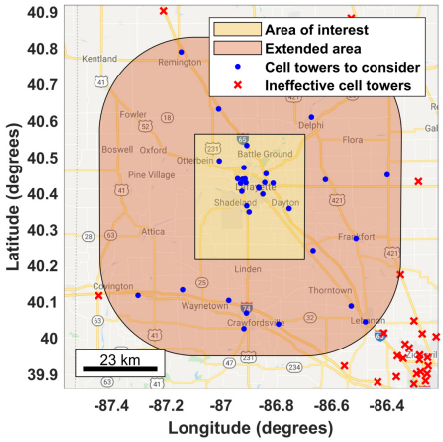

(a) For Tippecanoe County

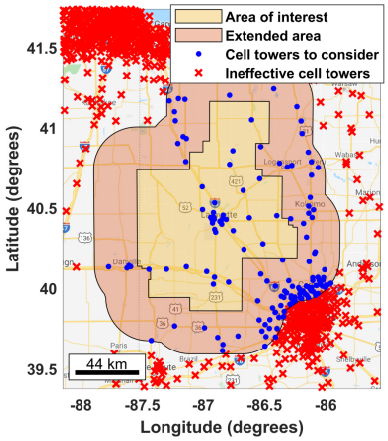

(b) For the WHIN area

Fig. 2. The area of interest is extended to filter out ineffective cell towers.

[1]Source code publicly available at: https://github.com/YaguangZhang/CellCoverageMapperForDronesMatlabWorkspace.git

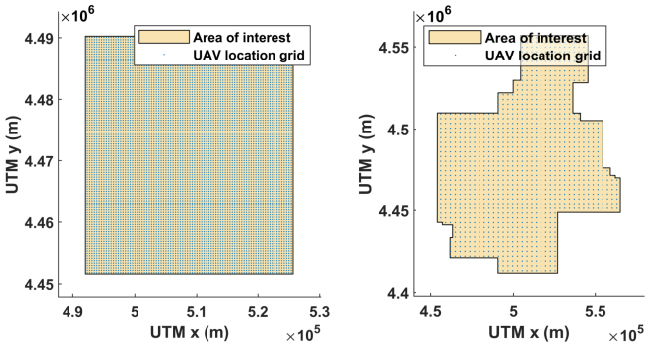

(a) For Tippecanoe County (b) For the WHIN area

Fig. 3. The UAV locations to be inspected are sampled evenly within the area of interest. (a) For Tippecanoe County, the grid has in total 8700 points with a spatial resolution of around 0.4 km. (b) For the WHIN area, the grid has in total 1249 points with a spatial resolution of around 2.9 km.

WHIN area, resulting in spacial resolutions of around 0.4 km and 2.9 km, respectively.

C. Blockage Map Generation

Blockage maps visualize locations with no clear LoS connection to any effective cell towers. Fig. 4 illustrates six as examples. Examining the figures, we observe that the blockage area decreases with increasing drone heights. Intuitively this makes sense, as higher altitude drones will more likely be operating above natural and man-made obstructions.

To determine blocked links, the Indiana 5-feet-resolution raster LiDAR dataset [12] was utilized in locating obstructions. At a given position, everything below the LiDAR z value (relative to the sea level) was assumed to be an obstruction. To improve accuracy, rather than computing blockage only along the direct path, we incorporated clearance tests for the first Fresnel zone. The first Fresnel zone provides a 3-dimensional (3D) ellipsoid surrounding the direct path; obstacles present in this zone will negatively influence the communication link. The radius of the first Fresnel zone $R_F(P)$ at any point P in between the endpoints of the link is given by:

$$R_F(P) = \sqrt{\frac{\lambda d_1 d_2}{d_1 + d_2}}, \quad d_1, d_2 \gg \lambda, \tag{2}$$

where d_1 is the distance of P from one end, d_2 is the distance of P from the other end, and λ is the wavelength of the transmitted signal. In the simulation, we set the signal carrier frequency $f_C = 1.9$ GHz to mimic a 4G LTE system operating in the Personal Communications Service band. For the purposes of computing blockage, a threshold of 60% clearance in the first Fresnel zone was set, the minimum value required for reliable wireless communication links [13].

To make large-scale analyses feasible, the clearance test was conducted via a 2-dimensional (2D) vertical plane, which contained the path connecting the cell tower antenna and the drone and intersected the first Fresnel zone in an ellipse, as illustrated in Fig. 5. Generating the blockage map then required constructing, for each effective cell tower antenna with each drone location in its R_{Max} range, a 2D obstacle profile based on the LiDAR data. For example, Fig. 5 illustrates the link

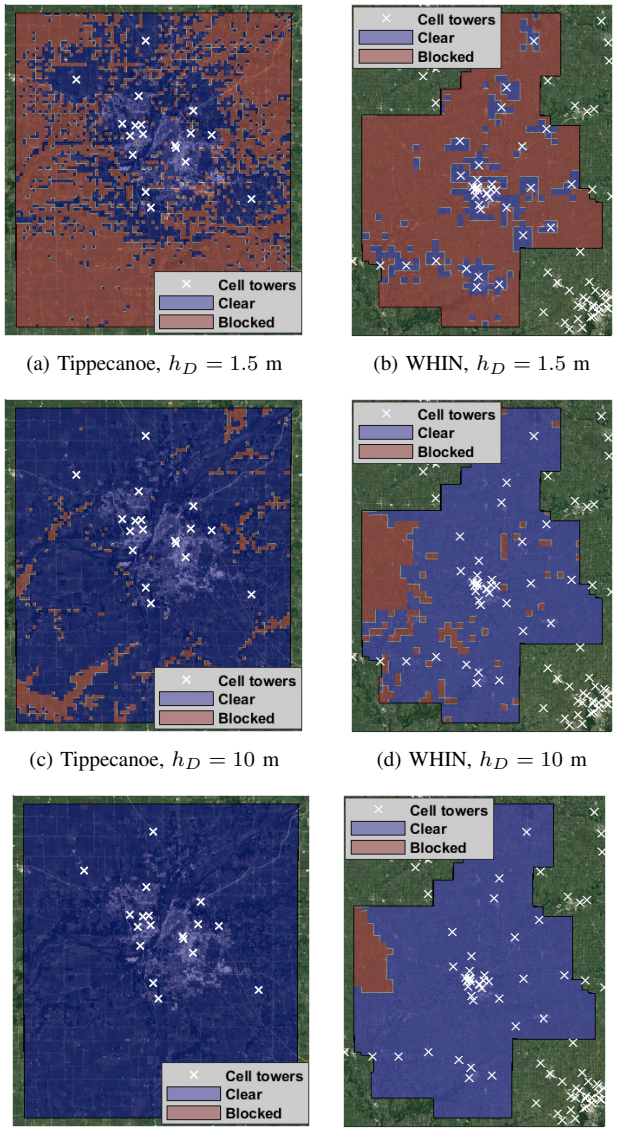

(a) Tippecanoe, $h_D = 1.5$ m (b) WHIN, $h_D = 1.5$ m

(c) Tippecanoe, $h_D = 10$ m (d) WHIN, $h_D = 10$ m

(e) Tippecanoe, $h_D = 100$ m (f) WHIN, $h_D = 100$ m

Fig. 4. Example blockage maps for Tippecanoe County and the WHIN area, with different drone heights. The blocked region shrinks dramatically as we increase the drone height from 1.5 m to 100 m.

between an effective cell tower (indicated by the cross mark) in WHIN and a nearby drone location to inspect (indicated by the solid circle). The top view also shows in dark grey the LiDAR data tiles, covering the whole Indiana State. The obstacle profile is generated by extracting a 2D vertical profile of LiDAR z values along the link of interest via bilinear interpolation. If the effective cell tower is located out of Indiana, profile samples may be out of the LiDAR dataset. For these locations, we fall back to the United States Geological Survey (USGS) 1/3rd arc-second terrain elevation data for the vertical profile values. The number of profile samples is set to be the minimum integer bigger than or equal to 10 that guarantees a spatial resolution smaller than or equal to 50 m. An obstacle LiDAR profile with this relatively large resolution may miss small-scale obstructions such as single trees, but

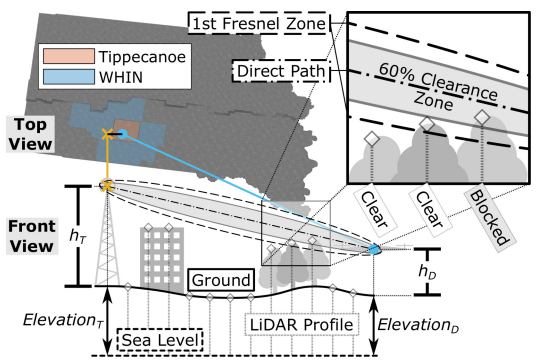

Fig. 5. Illustration showing the LoS path clearance test. An obstacle profile between the effective cell tower and the drone location is generated primarily from interpolating locally cached LiDAR and terrain elevation data for Indiana, as shown in the top view. Then, the 60% clearance test for the first Fresnel zone is carried out in the front view. In this example, the LiDAR sample for the rightmost tree indicates the LoS link is disrupted.

is necessary to limit the time required for simulations over such large geographic areas to a reasonable amount. Both the LiDAR data and the elevation data are cached locally for the whole Indiana State to further boost the simulation speed.

Once the profile has been extracted, the direct LoS path can be determined by the 3D coordinates UTM (x, y) and $altitude$ of the cell tower antenna and the drone position. If any of the obstacle LiDAR profile values are on or higher than the direct path, the LoS link is considered blocked. Otherwise, we will carry out the 60% clearance test for the first Fresnel zone demonstrated in Fig. 5. For each obstacle LiDAR profile point, we locate the corresponding P by intersecting the direct path with its perpendicular line which goes through that profile point. The LoS link is blocked if the distance from the profile point to the direct path is smaller than or equal to $0.6R_F(P)$. If the direct paths between the inspected drone location and all the effective cell towers are blocked, that location will be marked as "blocked" in the corresponding blockage map. This procedure helps improve the speed of the simulator by reducing the number of Fresnel zone calculations.

D. Path Loss Map Generation

The path loss maps are generated similarly to the blockage maps. However, instead of blockage indicators, they store at each drone location the best (minimum) available path loss for the links between all the effective cell towers and that drone location, as plotted in Fig. 6. In these maps, we can observe a clear decreasing trend for the path loss values as h_D is increased from 1.5 m to 100 m.

To estimate the median basic transmission loss using terrain elevation data, we utilized the NTIA C++ implementation [14] of the extended Hata (eHata) model [15]. The eHata model extends the applicability of the Hata empirical formula for the Okumura curves to 1500 MHz$\leq f_C \leq$3000 MHz with a transmitter-to-receiver (TX-to-RX) distance d between 1 km and 100 km. For $d < 1$ km, we computed the convex combination of the eHata result PL_{eHata} and the free-space path loss PL_{FSPL} via:

$$PL_{near} = \frac{d}{1 \text{ km}} \times PL_{eHata} + (1 - \frac{d}{1 \text{ km}}) \times PL_{FSPL}, \quad (3)$$

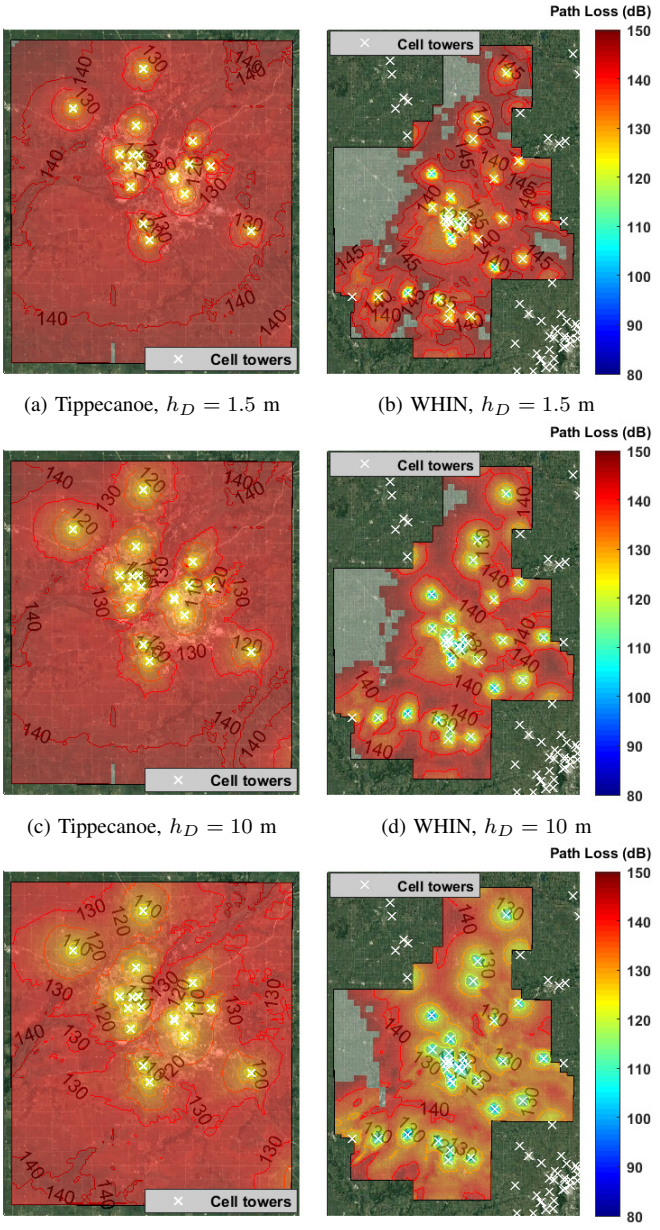

(a) Tippecanoe, $h_D = 1.5$ m (b) WHIN, $h_D = 1.5$ m

(c) Tippecanoe, $h_D = 10$ m (d) WHIN, $h_D = 10$ m

(e) Tippecanoe, $h_D = 100$ m (f) WHIN, $h_D = 100$ m

Fig. 6. Example path loss maps for Tippecanoe County and the WHIN area, with different drone heights. The region with path loss predictions lower than a specific value expands as we increase the drone height from 1.5 m to 100 m, implying improved communication conditions with relay UAVs.

where PL_{near} is the path loss for locations near the TX. The eHata model is designed for the case when the TX's altitude is larger than the RX's, so we assumed reciprocity and treated the higher one of the cell tower antenna and the drone to be the TX. The NTIA implementation also takes into account a set of site-specific adjustments based on terrain type and terrain elevation profiles. For simplicity, a fixed National Land Cover Database environment code of 82 (cultivated crops) was chosen in our simulator. The elevation profiles were generated in the same manner as the obstacle LiDAR profiles.

One advantage of considering path loss via channel modeling for large-scale coverage analyses is that the results are equipment-independent. With the huge range of devices at both

the cell tower and the user sides, it is practically difficult to collect the specifications for all the equipment involved over a large geographic area. Being the unavoidable major signal degradation contributor, path loss provides a fair coverage analysis without that information. However, the path loss values do not directly translate to a link quality indicator such as data rate; therefore it is necessary to compute link budgets with typical parameter values to form a connection between the path loss maps in the cellular coverage scenario and system-level key performance indicators. According to [16], for the downlink of a 4G LTE Frequency Division Duplex system, a user terminal typically has a noise figure of $NF_U = 9$ dB. With a bandwidth $B = 10$ MHz, the minimum detectable signal strength $MD_{DL} \approx -95$ dBm is given by:

$$MD_{DL} = 10 \times \log_{10}\left(\frac{kT}{1\text{mW}}\right) + NF_U + 10 \times \log_{10} B, \quad (4)$$

where k is the Boltzmann's constant and $T = 290$ K is the device temperature. Taking into account the typical cell tower antenna power $P_T = 64$ dBm, we have the maximum allowed path loss for the downlink $PL_{DL} \approx 177$ dB via:

$$PL_{DL} = P_T + G_T + G_U - MD_{DL}, \quad (5)$$

where $G_T = 18$ dBi and $G_U = 0$ dBi are the typical maximum antenna gains for the cell tower and the user terminal. Similarly, we can get the maximum allowed path loss for the uplink $PL_{UL} \approx 140$ dB, with the user terminal TX power $P_U = 23$ dBm and the noise figure for the cell tower $NF_T = 5$ dB. Note that the 140 dB PL_{UL} effectively sets the maximum coverage area for cellular communications. Thus, for the path loss maps, we set a threshold of $PL_{Max} = 150$ dB as the maximum allowed path loss value and discard any results above that. If the drone location does not have a lower or equal path loss value for any links originating from all the considered cell towers, the corresponding grid cell is considered out of service and will not be colored on the map, as shown in Fig. 6. Examining the figure, we observe a very poor coverage on the west side of WHIN. It is also worth noting that 140 dB of PL_{UL} is the typical worst uplink path loss for detecting the signal, which will not support good data connection links.

III. Coverage Analyses

Both the blockage and path loss maps in Fig. 4 and Fig. 6 have visually demonstrated promising cellular coverage improvement via data relay UAVs. Furthermore, we can easily obtain quantified results in terms of coverage area improvement from these maps. Fig. 7 presents the LoS coverage ratio, the ratio of the size for the clear region on the blockage map to the total size of the area of interest, at different UAV heights for Tippecanoe County and WHIN. For Tippecanoe County, a dramatic coverage gain over $90\% - 40\% = 50\%$ can be obtained by deploying UAV at $h_D = 10$ m, compared to a typical user terminal height of 1.5 m. For WHIN, that gain boosts to over 60%. Increasing the relay UAV beyond 10 m will further improve the LoS coverage, but with only an extra gain of around 10% for both cases.

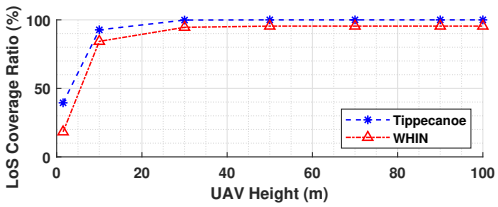

Fig. 7. Clear LoS coverage ratio based on blockage maps. A dramatic LoS coverage improvement can be achieved for both Tippecanoe County (over 50% gain) and WHIN (over 60% gain) by taking advantage of relay UAVs at a height of 10 m, compared to a typical pedestrian height of 1.5 m.

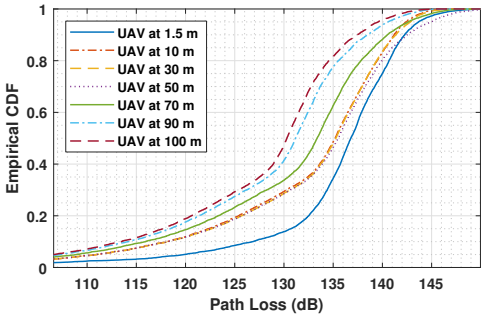

(a) Tippecanoe County

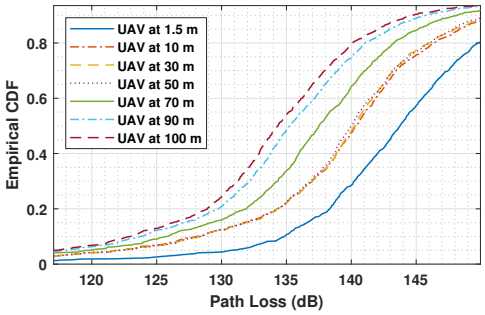

(b) WHIN

Fig. 8. Empirical CDFs for the path loss maps. With a given maximum allowed path loss value, we can find in these plots the corresponding coverage ratios for the UAV heights inspected.

Fig. 8 summarizes the path loss maps for all the UAV heights inspected with the empirical cumulative distribution functions (CDFs) of the path loss values stored in these maps. Because each path loss value represents a grid cell of a constant size on the corresponding map, the ratio of the path loss values small than or equal to a maximum allowed path loss PL_{Max} is the same as the coverage ratio for PL_{Max} in terms of area. That is, given PL_{Max}, we can directly use the empirical CDF values read from Fig. 8 as coverage ratios. For example, with $PL_{Max} = PL_{UL} = 140$ dB, we can get the coverage ratio for Tippecanoe County is around 75% at $h_D = 1.5$ m and around 95% at $h_D = 100$ m, yielding an improvement of $(0.95 - 0.75)/0.75 \approx 27\%$. Similarly, with $PL_{Max} = 140$ dB, we have for WHIN a coverage ratio of around 28% at $h_D = 1.5$ m and around 80% at $h_D = 100$ m, yielding a remarkable 186% improvement. The general rising trend of the curves with increasing h_D supports the use of relay UAVs. To better demonstrate these improvements, the coverage ratio gains relative to the $h_D = 1.5$ m case are plotted in Fig. 9. For Tippecanoe County, as we increase h_D

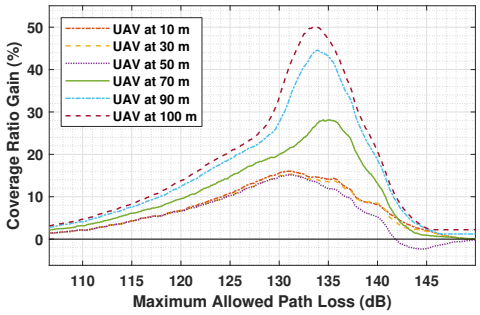

(a) Tippecanoe County

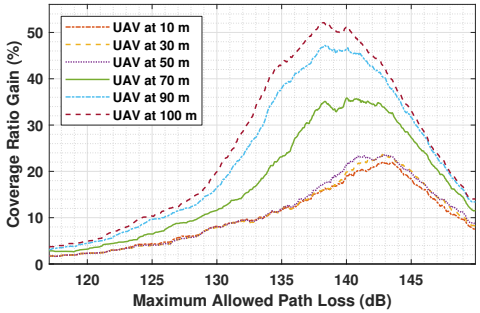

(b) WHIN

Fig. 9. Coverage ratio gain relative to the $h_D = 1.5$ m case.

from 10 m to 100 m, the coverage gain at $PL_{Max} = 140$ dB increases from 5% to 20%, while the whole region from 130 dB to 140 dB gets a significant boost with the highest gain of around 50% at 133.5 dB. This implies a moderate improvement for the worst acceptable coverage with a dramatic larger area getting better service. On the other hand, the WHIN area enjoys a significant boost between 130 dB and 140 dB, particularly at the high end with a gain from 19% to 51% as h_D increases, indicating a large area with no cellular service will get covered with relay UAVs.

We have focused on extending LTE cellular coverage for digital agriculture applications. However, the same methodology can be applied to other systems such as future millimeter-wave systems, where the blockage maps will play a more important role because of the high sensitivity of millimeter waves to blockage [17]. With more and more digital terrain data becoming available, our coverage analysis tool will be able to quantify the benefit of utilizing relay UAVs for more areas of interest. The biggest challenge for such a tool is to speed up the computation to cope with the large geographic area considered. The bottleneck of our algorithms is the LiDAR/elevation terrain profile generation because of the huge amount of data involved. Besides the techniques already mentioned, we also applied the following tricks to speed up the simulation: reprocess local data for indexes to enable faster search and data fetch; issue concurrent HTTP requests (up to 100 simultaneous threads via Python with MATLAB's two-way integration feature) for data not cached locally; reuse terrain profiles for different heights; use parallel computing and preassign tasks to workers to avoid frequent worker initialization. On a 36-core cluster with 216 GB RAM, the simulation for Tippecanoe County took two days and that for WHIN took less than a week.

IV. Conclusion

In this paper, we present algorithms to generate blockage maps and path loss maps via channel modeling for large-scale cellular coverage analyses on UAV data relay. Both visual and quantitative results are provided for Tippecanoe County and the ten counties in WHIN. According to these results, a significant coverage gain over 40% at a UAV height of 100 m is expected for both cases. These analyses are crucial in guiding the implementation of UAV data relay systems.

References

[1] S. Sekander, H. Tabassum, and E. Hossain, "Multi-tier drone architecture for 5G/B5G cellular networks: Challenges, trends, and prospects," *IEEE Communications Magazine*, vol. 56, no. 3, pp. 96–103, March 2018.

[2] B. Rao, A. G. Gopi, and R. Maione, "The societal impact of commercial drones," *Technology in Society*, vol. 45, pp. 83 – 90, 2016, doi: 10.1016/j.techsoc.2016.02.009.

[3] D. Zorbas, T. Razafindralambo, D. P. P. Luigi, and F. Guerriero, "Energy efficient mobile target tracking using flying drones," *Procedia Computer Science*, vol. 19, pp. 80 – 87, 2013, doi: 10.1016/j.procs.2013.06.016.

[4] M. Mozaffari, W. Saad, M. Bennis, Y. Nam, and M. Debbah, "A tutorial on UAVs for wireless networks: Applications, challenges, and open problems," *IEEE Communications Surveys Tutorials*, vol. 21, no. 3, pp. 2334–2360, thirdquarter 2019.

[5] N. Hossein Motlagh, T. Taleb, and O. Arouk, "Low-altitude unmanned aerial vehicles-based Internet of things services: Comprehensive survey and future perspectives," *IEEE Internet of Things Journal*, vol. 3, no. 6, pp. 899–922, Dec 2016.

[6] H. Menouar, I. Guvenc, K. Akkaya, A. S. Uluagac, A. Kadri, and A. Tuncer, "UAV-enabled intelligent transportation systems for the smart city: Applications and challenges," *IEEE Communications Magazine*, vol. 55, no. 3, pp. 22–28, March 2017.

[7] D. Murugan, A. Garg, and D. Singh, "Development of an adaptive approach for precision agriculture monitoring with drone and satellite data," *IEEE Journal of Selected Topics in Applied Earth Observations and Remote Sensing*, vol. 10, no. 12, pp. 5322–5328, Dec 2017.

[8] M. Mozaffari, W. Saad, M. Bennis, and M. Debbah, "Efficient deployment of multiple unmanned aerial vehicles for optimal wireless coverage," *IEEE Communications Letters*, vol. 20, no. 8, pp. 1647–1650, Aug 2016.

[9] Y. Chen, W. Feng, and G. Zheng, "Optimum placement of UAV as relays," *IEEE Communications Letters*, vol. 22, no. 2, pp. 248–251, Feb 2018.

[10] S. Zhang, Y. Zeng, and R. Zhang, "Cellular-enabled UAV communication: Trajectory optimization under connectivity constraint," in *2018 IEEE International Conference on Communications (ICC)*, May 2018, pp. 1–6.

[11] The Wabash Heartland Innovation Network consortium. About WHIN. Accessed: Oct. 28, 2019. [Online]. Available: https://whin.org/about/

[12] *IndianaMap (2011): IndianaMap Framework Lidar*. Indiana Statewide Imagery and LiDAR Program, distributed by OpenTopography, October 2012, doi: 10.5069/G9959FHZ.

[13] D. D. Coleman and D. A. Westcott, *CWNA: Certified Wireless Network Administrator Official Study Guide: Exam PW0-105*. John Wiley & Sons, 2012.

[14] National Telecommunications and Information Administration. The extended Hata (eHata) urban propagation model. Accessed: Oct. 24, 2019. [Online]. Available: https://github.com/NTIA/ehata.git

[15] E. F. Drocella, J. Richards, R. Sole, F. Najmy, A. Lundy, and P. McKenna, *3.5 GHz exclusion zone analyses and methodology*. US Department of Commerce, National Telecommunications and Information Administration, 2016.

[16] National Telecommunications and Information Administration. LTE (FDD) transmitter characteristics. Accessed: Oct. 24, 2019. [Online]. Available: https://www.ntia.doc.gov/files/ntia/meetings/lte_technical_characteristics.pdf

[17] Y. Zhang *et al.*, "Improving millimeter-wave channel models for suburban environments with site-specific geometric features," in *2018 International Applied Computational Electromagnetics Society Symposium (ACES)*, March 2018, pp. 1–2.